Environ. Sci. Technol. **2006**, *40,* 1485−1490

Influence of Copper Loading and Surface Coverage on the Reactivity of Granular Iron toward 1,1,1-Trichloroethane

STEPHEN J. BRANSFIELD,[†]
DAVID M. CWIERTNY,[‡]
A. LYNN ROBERTS,[‡] AND
D. HOWARD FAIRBROTHER*,[†,§]

Department of Chemistry, Department of Geography and Environmental Engineering, and Department of Materials Science and Engineering, Johns Hopkins University, 3400 North Charles Street, Baltimore, Maryland 21218

Although iron-based bimetallic reductants offer promise in treating organohalides, the influence of additive mass loading and two-dimensional surface coverage on reductant reactivity has not been fully elucidated. In this study we examine 1,1,1-trichloroethane reduction by Cu/Fe bimetals as a function of Cu loading and surface coverage. Information from a suite of complementary techniques (X-ray photoelectron spectroscopy, Auger electron spectroscopy, and cross-sectional energy-dispersive X-ray spectroscopy) indicates that displacement plating produces a heterogeneous metallic copper overlayer on iron. The dependence of pseudo-first-order rate constants (k_{obs} values) for 1,1,1-trichloroethane reduction on Cu loading exhibits two distinct regimes. At Cu loadings less than 1 monolayer equivalent (∼10 μmol Cu/g Fe), a pronounced increase in k_{obs} is associated with a corresponding increase in the two-dimensional surface *coverage* of Cu. A weaker dependence of k_{obs} on Cu mass is exhibited at loadings in excess of 1 monolayer equivalent, which we ascribe to an increase in the *volume* of the metallic overlayer. The observed relationship between k_{obs} and loading suggests that 1,1,1-trichloroethane reduction occurs on the Cu surface rather than at the interface between the Cu overlayer and the iron substrate.

Introduction

Despite the successes achieved (*1*) in treating organohalides with granular iron permeable reactive barriers (FePRBs), important limitations remain. For example, although iron reacts readily with many alkyl and vinyl polyhalides (*2*), certain species (e.g., dichloromethane, 1,2-dichloroethane) appear recalcitrant (*3*). Furthermore, some organohalides undergo only partial dehalogenation, leading to the accumulation of environmentally persistent byproducts. This is exemplified by the reduction of 1,1,1-trichloroethane (1,1,1-TCA) to 1,1-dichloroethane (1,1-DCA), a product that reacts, at best, slowly with iron (*4*).

One option for overcoming these shortcomings is to enhance the reactivity of granular iron by plating a second metal, hereafter referred to as the metal additive, onto the iron surface to generate a bimetallic reductant. Numerous studies (*4*−*8*) have illustrated that iron-based bimetals can increase both rates of organohalide reduction and the yield of fully dehalogenated products. Whereas previous studies (*9*, *10*) suggest that deactivation due to the accumulation of passive iron oxides on the particle surface could limit the utility of bimetallic reductants in FePRBs, emerging strategies for source zone control such as subsurface nanoparticle injection (*8*) could potentially benefit from the enhanced reactivity of these materials.

Before bimetallic reductants can gain acceptance as an alternative form of iron-based treatment, several practical issues must be addressed, many of which are related to the mass of additive deposited on iron (i.e., the additive loading). For example, additive loading can alter reductant reactivity (*5*, *7*, *11*), and may be an important factor in the costs associated with the production of bimetals. Furthermore, the potential for metal additive leaching into groundwater would also likely be a function of the additive mass deposited. Thus, additive loading could dictate the environmental acceptability of introducing bimetallic reductants to groundwater aquifers. Despite these practical considerations highlighting the importance of additive loading, quantitative relationships that might allow reactivity to be predicted from additive loading have not been thoroughly investigated.

An improved understanding of the relationship between additive loading and reactivity may also clarify certain aspects of the molecular-level phenomena responsible for the enhanced reactivity commonly exhibited by bimetallic reductants. For example, some researchers (*12*) have speculated that organohalide reduction by bimetals occurs primarily at the surface of the metal additive, while others (*13*) have postulated that electron transfer takes place at the interface between the additive and the iron substrate. The latter scenario would be expected to produce a well-defined maximum in reactivity at submonolayer additive coverages, in the regime where the number of interfaces between the metal additive and iron would reach a maximum.

In a noteworthy study, Kim and Carraway (*7*) explored the reactivity of Pd/Fe reductants toward trichloroethylene (TCE) as a function of Pd loading, while also examining structural characteristics of the deposited Pd overlayer. Batch studies revealed that as the Pd loading increased, so too did the surface-area-normalized rate constants (k_{SA} values) for TCE reduction. Although k_{SA} values increased monotonically over the range of Pd loadings studied, the rate of increase in k_{SA} decreased considerably at loadings in excess of 0.1 wt %. Limited point analyses of Pd/Fe grains conducted with scanning electron microscopy in conjunction with energy-dispersive X-ray spectroscopy (SEM-EDS) revealed that Pd deposition onto granular iron produced a heterogeneous Pd overlayer. The authors proposed that this uneven Pd distribution might be responsible for the nonlinear dependence of reductant reactivity on Pd loading, consistent with TCE reduction occurring primarily at the Pd surface. This hypothesis could be tested by examining the dependence of reductant reactivity on the two-dimensional surface coverage of Pd. Unfortunately, such a relationship could not be constructed by Kim and Carraway, as SEM-EDS is not inherently a surface sensitive technique.

Grenier et al. (*9*) investigated the influence of Ni surface coverage on the reactivity of Ni/Fe bimetals toward *cis*-dichloroethene (*cis*-DCE). In this study, rate constants for *cis*-DCE reduction were found to increase with 2-dimensional Ni surface coverage (measured using Auger electron spec-

* Corresponding author e-mail: howardf@jhu.edu; phone: (410) 516-4328; fax: (410) 516-8420.
[†] Department of Chemistry.
[‡] Department of Geography and Environmental Engineering.
[§] Department of Materials Science and Engineering.

10.1021/es051300p CCC: $33.50
Published on Web 01/26/2006

troscopy, a surface sensitive technique). However, additive loadings were not determined on a mass basis; as a result, the dependence of additive surface coverage on the Ni loading could not be explored. Without an understanding of how additive surface coverage changes as a function of additive loading, mechanistic insights pertaining to the location of *cis*-DCE reduction could not be deduced from this work.

In the present investigation, we examine the relationship between Cu loading and the reactivity of Cu/Fe bimetals toward 1,1,1-TCA, while also considering the interplay between Cu loading and surface coverage. This is accomplished using a suite of reductant characterization techniques (X-ray photoelectron spectroscopy (XPS), Auger electron spectroscopy (AES), and SEM-EDS) to obtain information on the elemental composition and structure of the Cu overlayer. AES provides a quantitative measure of two-dimensional Cu surface coverage on the iron particles (*14*), while XPS can identify the oxidation state of deposited Cu. This surface-specific information, coupled with additive loadings (determined from atomic absorption spectroscopy (AAS) analysis of plating solutions) and data pertaining to the rates and products of 1,1,1-TCA reduction (determined from batch studies), allows relationships between deposited Cu mass, Cu surface coverage, and reductant reactivity to be developed. Consequently, results from this investigation not only provide insight into practical issues related to bimetallic reductant design, but may also aid in identifying the location at which organohalide reduction occurs on bimetallic reductants.

Experimental Section

Reagents. Details pertaining to chemicals used in this study are provided in the Supporting Information.

Preparation of Cu/Fe Bimetals. Cu/Fe reductants were prepared within an anaerobic chamber (95:5 N_2/H_2) via displacement plating of Fisher electrolytic iron powder (100 mesh) with solutions of copper chloride. A detailed protocol for reductant preparation is provided in the Supporting Information. The majority of the experimental data were collected with reductants prepared from $CuCl_2$ plating solutions, although some reductants were prepared from CuCl solutions.

The mass of copper deposited during displacement plating (i.e., the copper loading) was calculated from the loss of copper ion in the plating solution following exposure to granular iron. Copper ion concentrations were measured using a Perkin-Elmer Aanalyst 100 atomic absorption spectrometer ($\lambda = 327.4$ nm with an air−acetylene flame). A plating efficiency of ∼99% was achieved for plating solutions with copper concentrations ≤0.01 M, although this value was lower for copper concentrations >0.01 M.

Specific surface areas of acid-washed iron powder and Cu/Fe reductants were determined via Kr−BET adsorption, using a Beckman Coulter SA3100 surface area analyzer. No variation in reductant surface area could be discerned with respect to Cu loading.

Batch Experiments. Batch experiments were conducted in deoxygenated, buffered aqueous solutions (50 mM tris-(hydroxymethyl)aminomethane (Tris) in 0.1 M NaCl, initial pH of 7.20). Reactors contained 1.6 g/L of either Cu/Fe or unamended iron, and an initial 1,1,1-TCA concentration of ∼100 μM. Experimental systems were assembled in an anaerobic chamber according to the procedure outlined in ref *15* and were initially free of headspace. The experimental protocol and analytical methods are identical to those described elsewhere (*4*, *15*).

We note that all reported concentrations have been corrected for possible partitioning into the headspace that developed in our batch systems over time, presumably resulting from water reduction to H_2. Concentrations were also corrected for dilution resulting from the addition of fresh buffer during reactor sampling. These corrections were performed as described by Cwiertny and Roberts (*15*). Carbon mass balances in all experiments were ≥85%.

XPS Analysis. For XPS characterization, freshly prepared Cu/Fe reductants were mounted onto stainless steel sample stubs using carbon tape, and were placed in a sealed container prior to removal from the anaerobic glovebox. The samples were then transported to the XPS instrument, and then quickly transferred to a fast load lock chamber (backfilled with an overpressure of nitrogen) prior to introduction into the XPS analysis chamber. Details of the XPS analysis can be found elsewhere (*16*). For Ar^+ sputtering experiments, a Φ 04-303 differentially pumped ion gun (4 keV, 25 mA) was operated at a gas pressure of 15 mPa, and the sputter rate was calibrated using a Si wafer with a known oxide thickness.

AES Analysis. The surface coverage of Cu on Cu/Fe reductants was determined using a Φ 610 scanning Auger microprobe. Cu/Fe reductants were mounted onto stainless steal stubs prior to analysis as described in our prior work (*9*). Preliminary AES experiments carried out using point analysis (electron beam size 0.2−1.0 μm) revealed that the surface composition of Cu/Fe reductants exhibited considerable spatial variability. Therefore, for each CU mass loading, we report an *average* 2-dimensional Cu surface coverage for our reductants, obtained from AES analyses of three separate 500 × 500 μm^2 regions on Cu/Fe powders.

To eliminate the contribution to the AES signal from the carbon tape on which the samples were mounted, copper surface coverages (% Cu) were calculated by comparing the atomic concentration of copper to the total metal concentration (Cu + Fe) (i.e., % Cu = Cu/(Cu + Fe) × 100). In this way, the Cu surface coverage (which represents a mole fraction concentration) can vary from 0% (unamended iron) to 100% (iron particles completely buried by a thick Cu overlayer), thereby providing a convenient metric of Cu surface coverage. Secondary electron images and AES maps of Cu and Fe on Cu/Fe reductants were also collected in separate experiments using a Φ 660 scanning Auger microprobe.

SEM-EDS Analysis. The Cu overlayer was also examined using SEM-EDS. Freshly prepared Cu/Fe grains were embedded in epoxy and mechanically ground and polished to expose cross-sections of reductant particles. Backscattered secondary electron maps and elemental maps of Cu and Fe were collected using a JEOL 8600 Superprobe. Details pertaining to this analysis are provided in the Supporting Information.

Results and Discussion

Characterization of Reductant Particles. XPS analyses of freshly prepared Cu/Fe reductants revealed the presence of both Cu^0 and Cu^I species at the surface (Figure S-1 of the Supporting Information). After Ar^+ sputtering, the Cu^I signal disappeared and both the Cu(2p) and Cu Auger regions were consistent with the presence of a metallic copper overlayer. The rapid loss of Cu^I from the surface after Ar^+ sputtering suggests that copper exists on the iron particles as Cu^0. We attribute the presence of Cu^I at the surface to trace oxidation during sample transfer into the XPS chamber (as described in the Supporting Information).

Figure 1a shows typical AE spectra of (i) unamended iron, as well as Cu/Fe reductants plated with (ii) 3 and (iii) 9 μmol Cu/g Fe, respectively. In each case, spectra represent the average of three separate 500 × 500 μm^2 areas. Figure 1a illustrates that the average Cu surface coverage increases with the total mass of Cu deposited. A secondary electron image of the grains plated with 9 μmol Cu/g Fe is shown in Figure 1b, while the corresponding scanning Auger elemental maps of Cu and Fe are shown in Figure 1c and d, respectively.

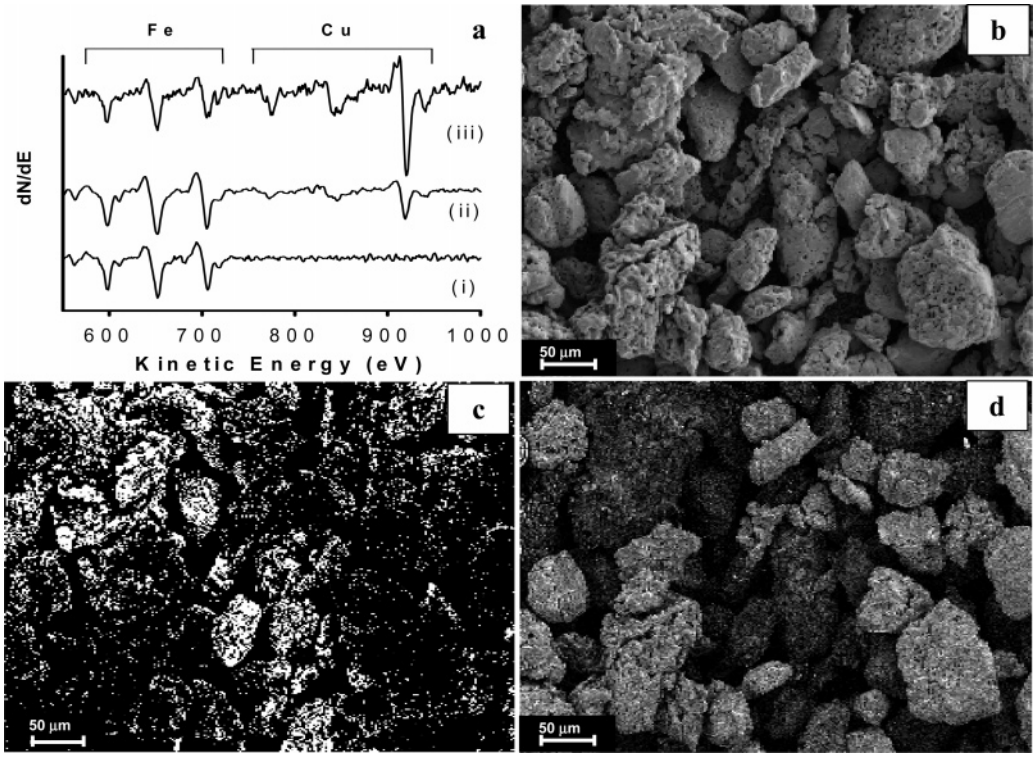

FIGURE 1. (a) Spectra obtained from scanning AES elemental maps of (i) unamended iron and Cu/Fe reductants with loadings of (ii) 3 and (iii) 9 μmol Cu/g Fe. All spectra have been normalized to the Fe peak at 598 eV. Only the AES regions above 550 eV (which include the Cu and Fe peaks located at 598 and 920 eV, respectively) are shown, although additional peaks due to oxygen (503 eV), carbon (271 eV), and chlorine (181 eV) were routinely observed during analysis. (b) Secondary electron image of iron grains plated with 9 μmol Cu/g Fe and the corresponding Auger maps of (c) Cu and (d) Fe obtained from the same Cu/Fe reductant in (iii). In (c), bright regions indicate areas of relatively high Cu surface concentration, while areas of relatively high Fe concentrations are shown as bright regions in (d).

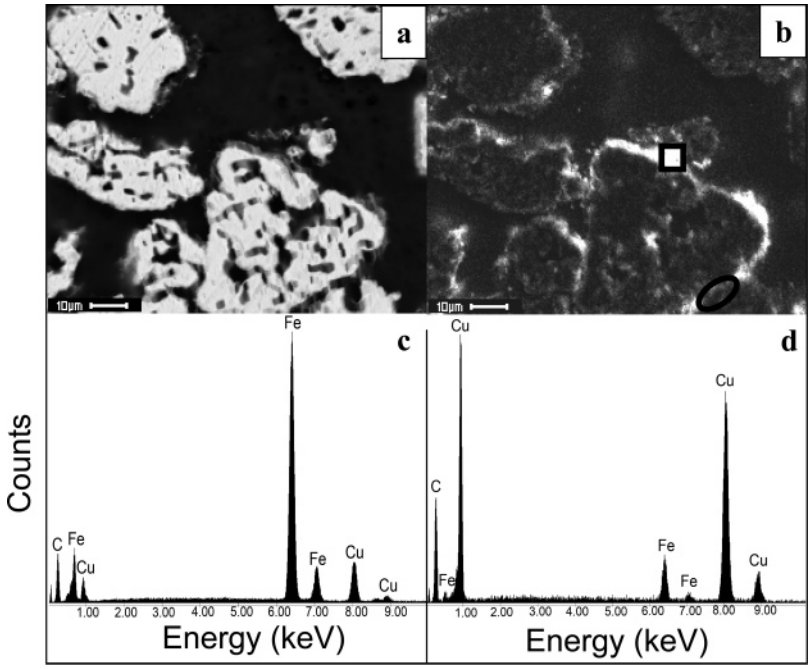

FIGURE 2. (a) Cross-sectional backscattered electron image of Cu/Fe particles with a loading of ~625 μmol Cu/g Fe. (b) Cu Kα X-ray map of the grains shown in (a), with bright regions indicating the presence of copper. (c) X-ray spectrum collected within the black oval. (d) X-ray spectrum collected within the black square.

These elemental maps reveal that the Cu distribution on the Fe surface is extremely heterogeneous.

The heterogeneous nature of the Cu overlayer suggested from AES analyses is supported by cross-sectional SEM-EDS analyses. An example is shown in Figure 2 for particles with a loading of ~625 μmol Cu/g Fe, corresponding to an average Cu surface coverage of 82% as determined by AES. The backscattered electron image obtained from cross-sectional analysis of these Cu/Fe particles is shown in Figure 2a, while 2b shows a Cu X-ray map of the same region. Even at this elevated Cu loading, some regions appear virtually free of deposited Cu. For example, the black oval in Figure 2b

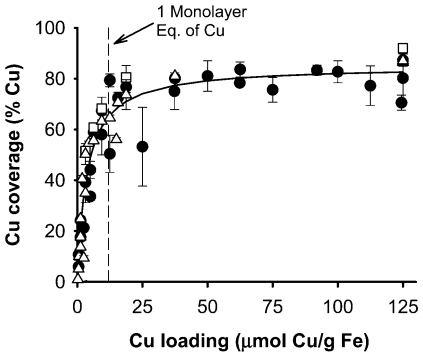

FIGURE 3. Plot of Cu surface coverage as a function of copper loading. The vertical dashed line indicates the estimated mass of deposited Cu equivalent to one monolayer Cu coverage. The solid black line represents a least squares nonlinear regression fit to all of the experimental data according to eq 1 ($R^2 = 0.980$), with α and γ equal to 85 (± 4.8) % Cu and 3.7 (± 0.9) μmol Cu/g Fe, respectively. Data are shown for reductants generated from aqueous $CuCl_2$ plating solutions (●) in the absence of added chloride, as well as from plating solutions containing $CuCl_2$ (□) or CuCl (△) in 1 M NaCl. AES values represent the average from analyses of three different subsamples of Cu/Fe reductant particles. Error bars represent one standard deviation in surface coverage determined via AES, while stated uncertainties in fitting parameters represent 95% confidence intervals.

highlights a region in which the amount of copper is very low (an X-ray spectrum collected within this region is shown in 2c). Conversely, regions exist on the same particle in which the copper overlayer appears several micrometers thick. One such region is within the black square in Figure 2b, for which the corresponding X-ray spectrum is shown in 2d. The heterogeneity of the Cu overlayer we observe for Cu/Fe reductants is similar to that reported by Kim and Carraway (*7*) for Pd/Fe reductants.

Relationship between Cu Surface Coverage and Cu Loading. Figure 3 shows the relationship between the average 2-dimensional Cu surface coverage (as determined by AES) and the Cu loading (as determined by AAS). Below roughly 5 μmol deposited Cu/g Fe, the copper surface coverage increases rapidly (and approximately linearly) up to a Cu surface coverage of approximately 60%. Above ~30 μmol Cu/g Fe, however, increases in the mass of deposited copper occur without substantial changes in the Cu surface coverage.

Cu surface coverage and mass loading proved insensitive to many experimental variables associated with the plating procedure used to generate Cu/Fe bimetals, such as the oxidation state of the copper salt and the chloride concentration in the plating solution. Rather, copper surface coverage appears to depend primarily upon the mass of Cu deposited (and hence, the concentration of the copper in the plating solution). Thus, data for reductants generated from CuCl solutions, as well as from $CuCl_2$ solutions with elevated NaCl concentrations (1 M), were indistinguishable from data collected with reductants generated from $CuCl_2$ solutions free of added chloride (Figure 3).

The relationship between the Cu surface coverage and the Cu loading is best described by the following hyperbolic expression (see Figure 3):

$$\%\ Cu = \frac{\alpha \cdot Cu_{mass}}{\gamma + Cu_{mass}} \qquad (1)$$

While empirical in nature, this expression illustrates the nearly linear increase in surface coverage at low values of Cu loading, and the essentially constant surface coverage observed at higher mass loadings.

A useful reference point in this relationship is the mass of Cu needed to plate the iron surface uniformly with 1 monolayer of Cu atoms (i.e., 1 monolayer equivalent). This theoretical loading was estimated by assuming that the Cu overlayer is predominantly in the lowest energy fcc (111) crystallographic orientation (*17*). Under these conditions, the surface area of one unit cell is given by

$$\textit{Surface Area of Unit Cell}\ (\mathrm{nm}^2) = 2 \cdot \sqrt{3} \cdot r^2 \qquad (2)$$

where r is the radius of a copper atom (0.128 nm) (*18*). Based on the measured specific surface area of the iron (0.4 ± 0.1 m^2/g), a single monolayer equivalent of Cu atoms would be obtained when ~10 μmol Cu/g Fe have been deposited on the Fe surface. This value is shown as a dashed vertical line in Figure 3.

Figure 3 demonstrates that the 2-dimensional Cu surface coverage reaches a maximum at a mass loading close to the value that corresponds to 1 monolayer equivalent of deposited Cu atoms. For Cu loadings below 1 monolayer equivalent, the rapid increase in Cu surface coverage is consistent with Cu deposition occurring predominantly onto the granular iron surface. The lack of increase in Cu surface coverage at loadings greater than 1 monolayer equivalent suggests that copper deposition at elevated loadings occurs predominantly onto metallic copper that has already been deposited.

Interestingly, a persistent iron signal was observed for every Cu/Fe reductant analyzed by AES. This suggests that the Cu overlayer is discontinuous, such that iron remains exposed at some fraction of the reductant surface, even at the highest Cu loadings considered in this investigation. Calculations outlined in ref *14* indicate that an Fe AES signal would only be observed if the Cu overlayer were thinner than ~5 monolayers. This value is substantially less than the average thickness of the Cu overlayer associated with the highest mass loading of Cu studied by AES (~60 monolayers). We cannot, however, entirely rule out the possibility of a continuous Cu overlayer that in some localized regions is sufficiently thin to allow a signal from the underlying iron substrate to be detected by AES.

Influence of Cu Loading on Reactivity toward 1,1,1-TCA. In agreement with a previous study (*4*), Cu/Fe bimetallic reductants proved more reactive than unamended iron toward 1,1,1-TCA. Over the experimental time scales (hours) studied in this investigation, no 1,1,1-TCA reduction was observed in batch reactors containing metallic copper powder in the absence of iron. Thus, although the addition of copper to the iron surface enhances the rate of 1,1,1-TCA reduction, iron is still necessary for reaction to occur.

Over the range of copper loadings investigated, addition of copper to the iron surface increased both the magnitude of the pseudo-first-order rate constants (k_{obs} values) for 1,1,1-TCA reduction and the yield of completely dehalogenated products relative to results obtained with unamended iron (Figure S-2 of the Supporting Information). For instance, the highest Cu loading for which rate constants were determined (125 μmol/g Fe) produced a 1,1,1-TCA half-life of 55 (± 3) minutes and roughly a 50% yield of ethane plus ethylene. In contrast, the half-life of 1,1,1-TCA in unamended iron systems was 220 (± 14) minutes, while ethane plus ethylene comprised only ~15% of the total product yield.

The relationship between k_{obs} and Cu loading is shown in Figure 4. The horizontal dashed line depicts the k_{obs} value obtained for reduction of 1,1,1-TCA by unamended iron (k_{obs} (Fe)). A pronounced increase in k_{obs} with increasing Cu loading is observed below 10 μmol Cu/g Fe, in the regime where we propose that Cu is deposited primarily onto the iron surface. At these low Cu loadings, the relationship between k_{obs} and deposited Cu mass appears linear. This

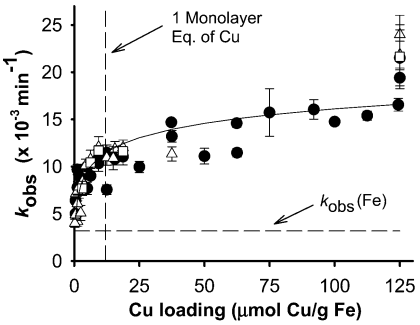

FIGURE 4. Influence of Cu loading on k_{obs} for 1,1,1-TCA reduction. The vertical dashed line indicates the estimated mass of deposited Cu equivalent to one monolayer Cu coverage. The horizontal dashed line denotes the k_{obs} value for 1,1,1-TCA reduction that was measured with unamended granular iron, k_{obs}(Fe). The solid black line represents a model fit to all of the experimental data, obtained by linear regression analysis of data transformed according to eq 3 ($R^2 = 0.967$), with m and b equal to 2.2 (± 0.35) × 10^{-3} min^{-1} and 5.9 (± 0.10) × 10^{-3} min^{-1}, respectively. Data are shown for reductants generated from aqueous $CuCl_2$ plating solutions (●), as well as from plating solutions composed of $CuCl_2$ (□) or CuCl (△) in 1 M NaCl. Uncertainties reported for fitting parameters indicate 95% confidence intervals, as do error bars shown for k_{obs} values.

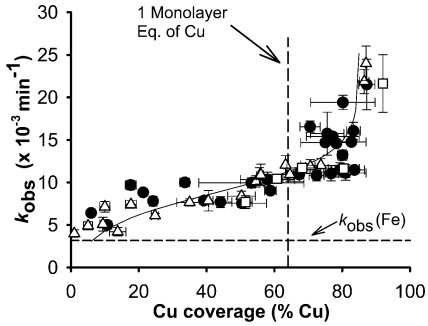

FIGURE 5. Effect of Cu surface coverage on k_{obs} for 1,1,1-TCA reduction. The horizontal dashed line denotes the k_{obs} value measured for 1,1,1-TCA reduction by unamended granular iron, k_{obs}-(Fe). The solid line represents the predicted values of k_{obs} as a function of % Cu determined by combining eqs 1 and 3. Data are shown for reductants generated from aqueous $CuCl_2$ plating solutions (●), as well as from plating solutions composed of $CuCl_2$ (□) or CuCl (△) in 1 M NaCl. For AES data, values represent the average determined from triplicate analyses of 3 different subsamples of Cu/Fe reductants. Error bars represent the 95% confidence interval for k_{obs} values and one standard deviation for AES measurements.

linearity is consistent with the findings of Wan et al. (*5*) for CCl_4 reduction at relatively low Pd loadings on iron (approximately 0.9−7 μmol Pd/g Fe).

Figure 4 also reveals a more modest rate of increase in k_{obs} at Cu loadings >10 μmol Cu/g Fe, corresponding to the region in which we hypothesize that Cu deposition occurs principally onto metallic Cu already present on the reductant surface. Thus, the majority of the rate enhancement provided by Cu/Fe appears to be associated with copper deposited directly onto the iron surface, although a smaller, additional rate enhancement is evident when thicker copper overlayers form at higher Cu loadings.

This dependence of k_{obs} on Cu loading was best described ($R^2 = 0.967$) by the following semilogarithmic relationship (see Figure 4):

$$k_{obs} = m \cdot \ln(Cu_{mass}) + b \quad (3)$$

A somewhat poorer agreement ($R^2 = 0.941$) was obtained when the experimental data were fit to a hyperbolic relationship of the kind used to describe the variation in Cu surface coverage as a function of Cu loading. This suggests that Cu surface coverage and k_{obs} exhibit different functional dependencies upon Cu loading; while Cu surface coverage plateaus at elevated Cu loadings, k_{obs} continues to increase (compare Figures 3 and 4). We note that the relationship between k_{obs} and Cu loading was independent of the oxidation state of Cu and the Cl^- concentration in the plating solution.

Interestingly, the highest Cu loading shown in Figure 4 (125 μmol Cu/g Fe) exhibits reactivity that is greater than would be anticipated from the empirical fit shown. This suggests that additional factors may influence Cu/Fe reactivity at very high Cu loadings. Nevertheless, these data reinforce the idea that the reactivity of Cu/Fe bimetallic reductants continues to increase at Cu loadings in excess of 1 monolayer equivalent.

Influence of Cu Surface Coverage on the Rate of 1,1,1-TCA Degradation. An alternative means of exploring the influence of Cu on granular iron reactivity is to examine the relationship between k_{obs} for 1,1,1-TCA reduction and copper surface coverage (Figure 5). The sharp increase in k_{obs} at Cu coverages greater than 1 monolayer equivalent is predicted from the empirical relationships previously presented in eqs 1 and 3. Combining these equations leads to an expression that directly relates k_{obs} for 1,1,1-TCA reduction to Cu surface coverage (% Cu)

$$k_{obs} = m \cdot \ln\left(\frac{\gamma \cdot \%\ Cu}{\alpha - \%\ Cu}\right) + b \quad (4)$$

The k_{obs} values predicted from measured Cu surface coverages using eq 4 (with values of α, γ, m, and b obtained as described above) are shown as the solid black line in Figure 5.

We interpret the sigmoidal nature of Figure 5 as evidence of two regimes in which the presence of copper accelerates iron reactivity toward 1,1,1-TCA. For Cu loadings below one theoretical monolayer, the increase in k_{obs} coincides with an increase in Cu surface coverage, and the predominant variable controlling Cu/Fe reactivity appears to be the two-dimensional copper coverage on the iron surface. In contrast, at Cu loadings above one theoretical monolayer, increasing k_{obs} values seem to result from the increasing mass of plated copper, as only small changes in the 2-dimensional copper coverage are observed at these higher loadings.

Implications for the Reactivity and Design of Bimetallic Reductants. The focus of this investigation was on the relationship between additive loading and surface coverage, and their influence on the reactivity of bimetallic reductants toward organohalides. Experimental evidence indicates that there is no Cu loading at which the value of k_{obs} is maximized with subsequent decreases in reactivity at higher loadings (see Figure 4). The monotonic increase in k_{obs}, even for Cu/Fe reductants whose surface is composed primarily of metallic copper, is consistent with the idea that 1,1,1-TCA reduction occurs predominantly at the surface of the additive, rather than at the interface between the additive and the granular iron substrate. Copper powder's lack of reactivity toward 1,1,1-TCA suggests that the granular iron particle serves as the primary source of reducing equivalents. Our proposed scenario for 1,1,1-TCA reduction therefore requires that reducing equivalents be transferred from the metallic iron core across the metallic copper overlayer to the surface where reductive dechlorination occurs.

From a practical perspective, results from this study suggest that a useful "target" additive loading may correspond to one monolayer equivalent of deposited Cu atoms. This mass would furnish the minimal Cu loading necessary to maximize the 2-dimensional Cu surface coverage on granular iron (Figure 3). Although k_{obs} values continue to increase at Cu loadings greater than one monolayer equivalent, the rate

of increase in k_{obs} per unit mass of additive decreases significantly.

One result that merits further investigation is the modest increase in 1,1,1-TCA reduction rates at elevated additive loadings (>10 μmol Cu/g Fe), in the regime where there is little or no change in the 2-dimensional surface coverage of Cu. No increase in the specific surface area of our reductant particles as a function of Cu loading could be discerned by Kr−BET. This suggests that increases in k_{obs} in this regime may be more indicative of a dependence of reactivity on the total *volume* of Cu deposited rather than on exposed Cu surface area. While we cannot rule out the possibility that Cu deposition produces changes in reductant surface area that are too small for detection by BET measurements, we note that some researchers (*13*, *19*) have proposed that *ab*sorbed atomic hydrogen, present as a product of water reduction (*20*), may represent a redox active entity responsible for organohalide reduction in bimetallic systems. Thus, the apparent role of additive volume in increasing k_{obs} may be a consequence of a developing copper lattice, which would be capable of serving as a reservoir for such a species.

The present study highlights the interplay between additive loading and two-dimensional surface coverage, as well as the influence of these parameters on the reactivity of bimetallic reductants. Both of these parameters are being examined in a study (*21*) designed to probe the effect of different metal additives (Au, Co, Cu, Ni, Pd, and Pt) on the reactivity of granular iron toward organohalides. Information from this investigation will enable us to identify the chemical and/or physical characteristics of the metal additives that are responsible for the rate enhancements typically observed with bimetallic reductants. As our Cu/Fe particles are likely to alter in surface composition as they "age" over time, another practical question relates to the influence of additive loading on the long-term reactivity of bimetallic particles toward organohalides, as well as the potential issue of additive leaching into groundwater. This question is currently being investigated in our laboratories using long-term column studies. Ultimately, such studies should provide information useful in the optimal design of bimetallic reductants from a perspective of cost, reactivity, and environmental impact.

Acknowledgments

We acknowledge Dr. Kenneth Livi (Department of Earth and Planetary Sciences) for assisting in the SEM/EDS analysis and Professor Peter Searson (Department of Materials Science and Engineering) for helpful discussions relating to this manuscript. We are also grateful for the comments of three anonymous reviewers, whose suggestions greatly improved this manuscript. Support for this research was provided by the National Science Foundation (CHE-0089168) as part of the Collaborative Research Activities in Environmental Molecular Science in Environmental Redox-Mediated Dehalogenation Chemistry at Johns Hopkins University. Additional funding for D.M.C. was provided by NSF and EPA graduate research fellowships.

Supporting Information Available

Information pertaining to the reagents used; the displacement plating method employed for preparation of bimetallic particles; XPS and SEM-EDS analyses of Cu/Fe bimetallic particles; and the effect of Cu loading on reactivity and product partitioning. This material is available free of charge via the Internet at http://pubs.acs.org.

Literature Cited

(1) *Field Applications of In Situ Remediation Technologies: Permeable Reactive Barriers*; EPA 542-R-99-002; U.S. EPA Office of Solid Waste and Emergency Response: Washington, DC, 2002.
(2) Johnson, T. L.; Scherer, M. M.; Tratnyek, P. G. Kinetics of halogenated organic compound degradation by iron metal. *Environ. Sci. Technol.* **1996**, *30*, 2634−2640.
(3) Puls, R. W.; Powell, R. M.; Blowes, D. W.; Vogan, J. L.; Gillham, R. W.; Powell, P. D.; Schultz, D.; Sivavec, T.; Landis, R. *Permeable Reactive Barrier Technologies for Contaminant Remediation*; EPA 600-R-98-125; U.S. EPA Offices of Research and Development and Solid Waste and Emergency Response: Washington, DC, 1998.
(4) Fennelly, J. P.; Roberts, A. L. Reaction of 1,1,1-trichloroethane with zerovalent metals and bimetallic reductants. *Environ. Sci. Technol.* **1998**, *32*, 1980−1988.
(5) Wan, C. H.; Chen, Y. H.; Wei, R. Dechlorination of chloromethanes on iron and palladium−iron bimetallic surface in aqueous systems. *Environ. Toxicol. Chem.* **1999**, *18*, 1091−1096.
(6) Kim, Y. H.; Carraway, E. R. Reductive dechlorination of TCE by zerovalent bimetals. *Environ. Technol.* **2003**, *24*, 69−75.
(7) Kim, Y. H.; Carraway, E. R. Dechlorination of chlorinated ethenes and acetylenes by palladized iron. *Environ. Technol.* **2003**, *24*, 809−819.
(8) Elliott, D. W.; Zhang, W.-X. Field assessment of nanoscale bimetallic particles for groundwater treatment. *Environ. Sci. Technol.* **2001**, *35*, 4922−4926.
(9) Grenier, A. C.; McGuire, M. M.; Fairbrother, D. H.; Roberts, A. L. Treatment of vapor-phase organohalides with zerovalent iron and Ni/Fe reductants. *Environ. Eng. Sci.* **2004**, *21*, 421−435.
(10) Muftikian, R.; Nebesny, K.; Fernando, Q.; Korte, N. X-ray photoelectron spectra of the palladium−iron bimetallic surface used for the rapid dechlorination of chlorinated organic environmental contaminants. *Environ. Sci. Technol.* **1996**, *30*, 3593−3596.
(11) Lin, C. J.; Lo, S. L.; Liou, Y. H. Dechlorination of trichloroethylene in aqueous solution by noble metal-modified iron *J. Hazard. Mater.* **2004**, *116*, 219−228.
(12) Schrick, B.; Blough, J. L.; Jones, A. D.; Mallouk, T. E. Hydrodechlorination of trichloroethylene to hydrocarbons using bimetallic nickel−iron nanoparticles *Chem. Mater.* **2002**, *14*, 5140−5147.
(13) Cheng, I. F.; Fernando, Q.; Korte, N. Electrochemical dechlorination of 4-chlorophenol to phenol. *Environ. Sci. Technol.* **1997**, *31*, 1074−1078.
(14) Vickerman, J. C., Ed. *Surface Analysis-The Principal Techniques*; John Wiley and Sons: Chichester, England, 1997; p 457.
(15) Cwiertny, D. M.; Roberts, A. L. On the nonlinear relationship between k_{obs} and reductant mass loading in iron batch systems. *Environ. Sci. Technol.* **2005**, *39*, 8948−8957.
(16) Wagner, A. J.; Wolfe, G. M.; Fairbrother, D. H. Reactivity of vapor-deposited metal atoms with nitrogen-containing polymers and organic surfaces studied by *in situ* XPS. *Appl. Surf. Sci.* **2003**, *219*, 317−328.
(17) Attard, G.; Barnes, C. *Surfaces*; Oxford University Press: Oxford, 1998; Vol. 59.
(18) Silberberg, M. S. *Chemistry: The Molecular Nature of Matter and Change*, 2nd ed.; McGraw-Hill: Boston, MA, 2000.
(19) Odziemkowski, M. S.; Gillham, R. W. Electroless Hydrogenation of Trichloroethylene by Fe−Ni(P) Galvanic Couples. In *Environmental Issues in the Electronics/Semiconductor Industries and Electrochemical/Photochemical Methods for Pollution Abatement*; Fenton, J. M., Ed.; The Electrochemical Society, Inc.: Pennington, NJ, 1998; pp 91−97.
(20) Reardon, E. J. Anaerobic corrosion of granular iron: measurement and interpretation of hydrogen evolution rates. *Environ. Sci. Technol.* **1995**, *29*, 2936−2945.
(21) Cwiertny, D. M., *Mechanistic Investigations of Granular Iron and Iron-Based Bimetallic Reductants for Treatment of Organohalide Pollutants.* Ph.D. Thesis, Johns Hopkins University, Baltimore, MD, 2005; pp 79−122.

Received for review July 5, 2005. Revised manuscript received December 5, 2005. Accepted December 6, 2005.

ES051300P